CONF-851007--13

RECEIVED BY OSTI OCT 09 1985

BNL-NUREG-37037

EVALUATION OF BWR EMERGENCY PROCEDURE GUIDELINES FOR BWR ATWS USING RAMONA-3B CODE*

L. Neymotin, G. Slovik, E. Cazzoli, and P. Saha
Brookhaven National Laboratory
Upton, New York 11973

BNL-NUREG--37037

TI86 000630

ABSTRACT

An MSIV Closure ATWS calculation for a typical BWR/4 (Browns Ferry, Unit 1) was performed using the RAMONA-3B code which is a BWR systems transient code combining three-dimensional neutronic core representation with multi-channel one-dimensional thermal hydraulics. The main objective of the study was to perform a best-estimate evaluation of the recently proposed Emergency Procedure Guidelines for Anticipated Transients Without Scram (ATWS). Emphasis was placed on evaluating the effects of lowering the downcomer water level to the Top of Active Fuel (TAF) and vessel depressurization.

The calculation was run up to approximately 1200 seconds. Both actions, namely, lowering the water level and vessel depressurization, lowered the reactor power to some extent. However, the pressure suppression pool water temperature still reached approximately 90°C (potential High Pressure Coolant Injection (HPCI) pump seal failure temperature) in twenty minutes. Thus, other actions such as boron injection and/or manual control rod insertion are necessary to mitigate a BWR/4 Main Steam Isolation Valve (MSIV) closure ATWS.

INTRODUCTION

Anticipated transient without scram (ATWS) is known to be a dominant accident sequence for possible core melt in a Boiling Water Reactor (BWR). A recent Probabilistic Risk Assessment (PRA) analysis (1) for the Browns Ferry, Unit 1, nuclear power plant indicates that ATWS is the second most dominant transient for core melt in a BWR/4 with Mark I containment, the most dominant sequence being the failure of long term decay heat removal function of the Residual Heat Removal (RHR) system. Therefore, a great deal of analysis has already been performed to understand the BWR behavior during an ATWS. References (2 - 5) provide some examples of earlier work.

Much work has also been done to prevent and mitigate any adverse consequences of an ATWS. Recirculation pump trip and boron injection are two prominent mitigative actions. In addition, the BWR owner's group has recently suggested that in the event of an ATWS, the operator should reduce the safety injection flow rate so that the downcomer water level drops from the normal level to the top of active fuel (TAF) and remains there. This new emergency procedure guideline (EPG) would lower the core flow rate, resulting in an increased core-average void fraction and a decreased reactor power. A lower reactor power would reduce the steam generation in the core and would eventually reduce the heat-up rate of the pressure suppression pool (PSP). Even then, the reactor vessel may have to be depressurized by manual control of the safety/relief valves as the PSP water temperature starts to increase beyond a certain limit. This action should also increase the core void fraction and help lowering the reactor power.

Analyses (6 - 11) have been performed to determine the reactor power assuming that the operator maintains the water level at TAF and depressurizes the reactor vessel in accordance with the new EPGs. However, the results of these analyses are very sensitive to the methodology used; sometimes the predicted power levels differ from one another by a factor of two. The objective of this study is, therefore, to perform a best-estimate calculation using one of the most sophisticated ATWS analysis tools presently available.

In a BWR, the vapor void fraction varies significantly in space, particularly in the vertical (or axial) direction. Because of strong void-reactivity feedback, a space-time neutron kinetics coupled with an adequate thermal hydraulic model is necessary for ATWS-type analysis where the axial power distribution is expected to vary significantly with time. Therefore, the RAMONA3B code (12) with three-dimensional neutron kinetics and one-dimensional, multi-channel, four-equation, thermal-hydraulics was chosen for the present study. It is expected that this study will provide the benchmark-type calculations which may be used to adjust the "simpler" analytical tools such as the BWR-LACP code (10).

BRIEF DESCRIPTION OF RAMONA-3B

RAMONA-3B has been developed at Brookhaven National Laboratory under the sponsorship of the U.S. Nuclear Regulatory Commission for analyzing BWR core and systems transients. The code employs a three-dimensional neutron kinetics model coupled with one-dimensional, four-equation, nonhomogeneous, nonequilibrium thermal hydraulics. To be compatible with 3-D neutron kinetics, the code uses parallel coolant channels in the core. It also includes a boron transport model and all necessary BWR components such as jet pump, recirculation pump, steam separator, steam line with safety and relief valves, main steam isolation valve, turbine stop valve and turbine bypass valve. An additional condensation model pertinent to condensation on cold safety injection water in the downcomer region has recently been implemented into the code, and is discussed in the Appendix.

*Work done under the auspices of the U.S. Nuclear Regulatory Commission.

The Appendix also includes a brief description of the RAMONA-3B neutronics and thermal-hydraulics modeling.

TRANSIENT SCENARIO

The transient presented in the paper was assumed to be initiated by an inadvertent closure of all MSIVs in the Browns Ferry plant starting at the full power corresponding to the end of Cycle 5 (Table 1). As a result, pressure in the reactor vessel rapidly increased causing a collapse of voids in the core with simultaneous increase in reactor power. The SRVs were assumed to operate as designed and the recirculation pumps were tripped upon reaching the high pressure set point (7.83 MPa with 0.53 sec delay). The feedwater was lost by 8 seconds and the plant was left in an automatic mode of operation until 150 seconds. At this time, operator recognized that an MSIV closure ATWS was in progress and started to act according to the Emergency Procedure Guidelines, i.e., the downcomer water level was gradually lowered to the TAF level. At the same time, the reactor vessel was depressurized to avoid excessive SRVs cycling.

Lowering the water level was accomplished by reducing the HPCI and RCIC flow rates. The safety injection systems were activated by a low water level signal earlier in the transient. This level was approximately 2.7 meters above the TAF elevation. Thereafter, the downcomer water level was kept at TAF by controlling the HPCI and RCIC injection flow rates until the end of the transient calculation. Along with the level control, another safety feature exercized by the plant operator was modeled in the calculation: the reactor pressure vessel was depressurized according to the PSP heat capacity temperature limit curve. It should be noted that the present transient scenario did not include such mitigating measures as boron injection or manual rod insertion. The sequence of events including some important system parameters is shown in Table 2.

INPUT MODEL

Neutronics Data and Core Modeling

The neutronic data used to model the core was generated from the state of Cycle 5 of Browns Ferry reactor at a core average burnup of 8876 MWD/MT. Tennessee Valley Authority (TVA) supplied a complete description of the core.

The analysis showed that 5 basic fuel types had to be calculated by CASMO (13) (a 2-D transport code) to supply the macroscopic cross sections required for the calculation of the state of the core as a function of exposure and void history. The grid used for each fuel type for each CASMO calculation set can be seen in Figure 1.

The overall scheme to process the cross sections is shown in Figure 2. After the macroscopic cross sections are defined by CASMO, the BLEND2 code (which has been developed at BNL) takes the exposures and void histories obtained from the TVA process computer for each node and determines the corresponding cross section set in the BNL-TWIGL format (14):

$$\Sigma(\alpha, T_m, T_F, F \mid E, V) = F(a+b\alpha+c\alpha^2) + (1-F)(a'+b'\alpha+c'\alpha^2) + P(T_m - T_m^*) + R(\sqrt{T_F} - \sqrt{T_F^*}) \quad (1)$$

Once each node is assigned its cross section set, BLEND2 performs a constrained minimization process using the exposure and void history of each node to group members of a fuel type (a group is called a chain) using the criteria

$$|E_i - E_j| < \delta E$$

$$|V_i - V_j| < \delta V,$$

where E_j, V_j, are the characteristics of a node arbitrarily chosen as a chain head and E_i, V_i are the properties of an element or chain head of another group to determine whether the j-node falls within the acceptance criteria determined by δE and δV. Several sweeps are made with increasing values of δE and δV until BLEND2 arrives at a predetermined total number of cross section sets. The cross section set number and its corresponding node location are printed out by BLEND2 (the cross sections are automatically created in the RAMONA-3B format) to create a RAMONA-3B core model.

In order to test the RAMONA-3B performance in simulating the reactor steady state condition, the TVA-supplied axial power distribution at the end of fuel cycle 5 along with the corresponding operating conditions was used. This EOC-5 condition at E = 8876 MWD/MT was chosen because it corresponds to the most reactive state of the core during an ATWS as the control rods are almost completely withdrawn.

The BLEND2 code was run twice: once to get a set of 13 cross sections which had the final selection criteria of δE = 5291 MWD/MT and δV = 0.39, and second, to produce a 20 cross section set with the final selection criteria of δE = 4233 MWD/MT and δV = 0.31. The two different cross section sets were generated to perform a sensitivity study on the effects of exposure and void history on the cross sections sets.

The RAMONA-3B steady state calculations were performed using a 1/8 core representation with 101 neutronic and 9 hydraulic channels with 24 axial levels (2424 neutronic and 216 hydraulic nodes). The results obtained by using the two above-mentioned cross section sets, i.e., 13 and 20 cross section sets in each, to predict the TVA steady state operating condition can be seen in Figure 3. Both predictions are in good agreement with the data which indicates that the two cross section sets developed for EOC-5 are not overly sensitive to the exposure and void history selection criteria (δE and δV). Therefore, the cross sections with 13 sets were selected for use in the present calculation.

To determine the optimum number of nodes sufficient for accurate modeling of the core, a study was performed with the following four core nodalization options (all with 101 neutronic channels):

9 hydraulic channels and 24 axial levels - reference case, 9 channels with 12 levels, 7 channels with 12 levels, and 7 channels with 10 levels. All calculations were run up to 70 seconds for an MSIV closure ATWS scenario. Based on the results of this study, the 7 hydraulic channels with the 10 axial level nodalization scheme was chosen for the ATWS calculation presented in this paper.

Plant Modeling (Thermal Hydraulics)

The RAMONA-3B representation of a BWR pressure vessel (Fig. 4) includes a downcomer, lower plenum, core, riser, steam separator and the steam dome with steam lines. Each steam line is equipped with the MSIV, SRVs and TBVs. The feedwater spargers are located in the upper part of the downcomer, whereas the jet pumps and the recirculation loops are associated with the lower part of the downcomer region. Eleven hydraulic cells were used to model the one-dimensional thermal-hydraulics of the downcomer.

The lower plenum was modeled with five hydraulic cells and was coupled with seven parallel hydraulic channels representing the reactor core region. Six of them were heated channels (in-bundle region) and the seventh was the core integral bypass channel. All channels were modeled with 10 hydraulic cells and the 1/8 symmetry core option was used in the calculation assuming that an 1/8 slice of the core was representative of the whole core. The assumption was based on evaluations of the Browns Ferry Cycle 5 core map obtained from TVA.

The one-dimensional riser (including the upper plenum) was connected with the core exit and was modeled using five hydraulic cells. Finally, based on a nodalization study, six hydraulic cells were used in the steam line between the steam dome and the MSIV.

Four banks of SRVs were modeled (each having specific pressure set points (Table 3)) in the steam lines. It should be noted that the vessel depressurization curve (pressure as a function of the PSP bulk water temperature) was imposed on the calculation by appropriate continuous adjustment of the SRV set points.

CALCULATION RESULTS

Selected results of the calculation are shown in Figures 5 through 13. Since the objective of the paper is evaluation of the Emergency Procedure Guidelines, we will start the discussion from the calculation results associated with the plant conditions imposed by the EPGs. As mentioned in the introduction, the major procedure is lowering and keeping the downcomer water level at the top of active fuel (TAF). As a result of this action, a drop in the reactor power was expected due to decrease in the core flow rate (because of decrease in the driving head) followed by an increase in the core void fraction (negative void reactivity feedback).

It can be seen in Figure 5 that the water level is dropping from the beginning of the transient due to loss of water inventory (SRVs are open and combined HPCI and RCIC capacity is not sufficient to replenish the water inventory). The rate of the level drop considerably increases when the operator assumes control of the plant and reduces the safety water injection rate. The water level reaches the TAF elevation at about 240 seconds and is kept there till the end of the transient.

The operator actions are more clearly depicted in Figure 6 showing the SRV flow rate (mass leaving the vessel) and the feedwater or HPCI and RCIC flow rate (mass entering the system), thus reflecting the vessel inventory as well as the water level histories. (Note that the anticipated reduction of S/RV cycling resulting from the vessel depressurization was predicted very well between 150 and 400 seconds). Results shown on this figure suggest that matching the SRV and ECC flow rates would be an ideal way of maintaining the water level at a desired elevation.

It is worthwhile at this point to mention that RAMONA-3B has a model to specifically represent condensation of steam on cold safety injection water (see Appendix). Since this water is injected through the feedwater spargers, the condensation starts as soon as the downcomer water level drops below the sparger elevation. The condensation model takes into account condensation on cold water jets (96 jets each of 44 mm diameter in the present calculation) and on the downflowing water film that is composed of the water exiting from the steam separators and injected ECC water. The film may be either subcooled or saturated depending on the condensation rate on the cold water jets.

An important system parameter affected by the condensation in the upper downcomer region is the water subcooling at the core entrance. The reactor power is sensitive to the core inlet subcooling through the moderator temperature and void reactivity feedbacks. As seen from Figure 5, after approximately 50 seconds from the initiation of the transient, the highly subcooled water was being injected into the pure steam environment. So the core inletsubcooling as shown in Figure 7 becomes a function of the steam separator water return flow, ECC water temperature and injection flow rate and the condensation rate. By 20 minutes of the transient, the subcooling of the core inlet was approximately 10°C (18°F).

As expected, immediately after the MSIV closure initiation, the reactor vessel pressure experienced a rapid increase (Figure 8) followed by a void collapse in the core (Figure 9) (the large time scale in the figures does not allow for adequate resolution in this time domain). The latter introduced a positive reactivity insertion and a rapid increase in the power in the first four seconds of the transient. By approximately 35 seconds, the system pressure dropped to the level of the relief valves set points and started to oscillate following the SRV cyclings. At 170 seconds, the vessel was manually depressurized, and from then on, the pressure was kept below the limit imposed by the PSP heat capacity temperature limit curve.

The reactor core response to the initial pressure increase was a power spike with the total power reaching about 256% of the nominal value at 2.6 seconds. Subsequent core voiding caused by the combination of the SRV openings and a drop in the

core flow rate caused by the recirculation pump trip, brought the power to approximately 30% level (Figure 10). From then on, until the operator assumed control of the plant at 150 seconds, the power was oscillating concurrently with oscillations in the system pressure (and voids in the core) produced by actions of the SRVs.

The core flow rate shown in Figure 11 is one of the major power controlling parameters in the transient. The early drop in the core flow rate was due to the recirculation pump trip. Thereafter, the objective of the EPG was to further decrease the core flow rate during the natural circulation mode by lowering the downcomer water level to TAF. The effect of this operator action, started at 150 seconds, can be seen until approximately 250 seconds when a quasi-steady state flow rate was reached. Since then the core flow rate remained in the vicinity of 16% of the nominal steady state value. As it was expected, the reactor power (Figure 10) also dropped following the reduction in the core flow rate.

The slight increase in power which started at about 270 seconds can be explained in terms of the core inlet subcooling (Figure 7). By that time the cold water injected by the ECC system arrived at the core inlet causing a positive reactivity insertion in the core. From that time on, the reactor power, governed primarily by the core flow rate, inlet subcooling, and system pressure, was gradually decreasing. By 1160 s, the power reached approximately 17% of the steady-state value. The combined effect of the governing parameters is shown in Figure 12 where different components of the core reactivity are plotted as a function of time. It is seen that the positive reactivity insertion due to the Doppler and moderator temperature effects (system pressure is decreasing so that the fuel and moderator temperatures decrease also) is balanced by the negative void reactivity feedback due to void increase (see the corresponding plot of the core average void history in Figure 9). It can also be seen from the reactor pressure and power plots (Figures 8 and 10) that with the water level at TAF, a continuous vessel depressurization produced roughly 1% drop in power per every 100 psi (7 bar) drop in pressure.

Since the main objective of the EPGs is to maintain the containment integrity while bringing the reactor to a hot shutdown, condition of the PSP is an important safety parameter. Because of the steam discharged through the SRVs into the PSP, the pool water temperature starts to rise. To maintain the containment integrity, it is important to keep the PSP water temperature at a sufficiently low value. In the present study this temperature was calculated by a simple, stand-alone computer program written to solve the mass and energy conservation equations for the suppression pool water. Steam flow rates and enthalpies calculated by RAMONA-3B were used as input to this program. Complete condensation of steam in the pool water was assumed and no credit for the pool cooling by the RHR system was taken.

The result produced in the latter calculation is shown in Figure 13. It can be seen that the PSP temperature does reach ~190°F (88°C) at the end of the predicted transient (dashed line indicates the potential HPCI failure temperature; HPCI pumps are cooled by the PSP water). Consequently, the HPCI pumps failure would lead to a loss of inventory and potential core uncovery. Thus, the effects of other mitigative features such as manual rod insertion and use of Standby Liquid Control System (SLCS or boron injection) must also be considered for ATWS analysis.

DISCUSSION AND CONCLUSIONS

The results presented above show that the events governing the total reactor power, which is the main global safety parameter, are the changes in the system pressure, core inlet subcooling and the core flow rate. Combined effect of these three thermal hydraulic parameters controlled the reactor power mainly through the mechanism of void reactivity feedback. On the other side, the Doppler effect and lower moderator temperature were the main contributors into the total core reactivity balance.

Results obtained in this study are quite close to those obtained by EPRI and its contractors (6-8) using space-time neutron kinetics. The present study also showed significant changes in the axial core power distribution with time which affect the void distribution, core flow rate, core-average void fraction, and, consequently, the reactor power. Thus, a point-kinetics model, which is unable to capture the changes in the power distribution, is not reliable for predicting the reactor power during an ATWS event. However, recent BNL studies [15] showed that a one-dimensional (axial) neutron kinetics can be successfully used in ATWS calculations if the core's radial symmetry is preserved with time.

The following conclusions are drawn from the present study on MSIV closure ATWS for Browns Ferry, Unit 1, plant:

1. Lowering the water level to the top of active fuel (TAF) during a BWR ATWS event would help in reducing the reactor power to some extent (e.g., to ~20% of steady-state power). However, this benefit is significantly less than what was perceived during the formulation of the new Emergency Procedure Guidelines (EPGs).

2. Vessel depressurization according to the pressure suppression pool (PSP) heat capacity temperature limit curve also helps lowering the reactor power to some extent (e.g., ~1% reduction in power for every 100 psi drop in pressure, as seen from Figures 8 and 10). However, even with the combination of level and pressure control, the PSP bulk water temperature could reach ~190°F (88°C) in twenty minutes. Thus, other mitigative actions such as boron injection and/or manual rod insertion must be used to prevent any core or containment damage.

3. RAMONA-3B with space-time neutron kinetics is very useful in predicting the best-estimate behavior of BWRs during an ATWS event where the core power distribution significantly varies with time. If desired, these RAMONA-3B results can be used to benchmark point-kinetics codes for scoping calculations.

ACKNOWLEDGMENTS

The Authors would like to thank Bharat B. Agrawal of the USNRC for his comments and suggestions during this work. Special thanks to Steve Hodges and Mike Harrington of ORNL for their helpful discussions, to Peter Kohut of BNL for running the CASMO code and to Helen C. Connell of BNL for her computer support. Discussions with several INEL and TVA staff members are also gratefully acknowledged. Finally, the fine typing by Ms. Ann C. Fort is highly appreciated.

REFERENCES

(1) S.E. Mays, et al., "Interim Reliability Evaluation Program: Analysis of Browns Ferry 1, Unit 1, Nuclear Plant," NUREG/CR-2802, EGG-2199, July 1982.

(2) A. Aronson, et al.,"Status Report on BNL Calculations of ATWS in BWR's," BNL-17608, RP 1022, 1973.

(3) General Electric Company, "Assessment of BWR Mitigation of ATWS," Vol. II, (NUREG-0460 Alternate No. 3), NEDO-24222, February 1981.

(4) C.J. Hsu, L. Neymotin and P. Saha, "Analysis of a Typical BWR/4 MSIV Closure ATWS Using RAMONA-3B and TRAC-BD1 Codes," ASME Paper No. 84-NE-10, presented at the Joint ANS/ASME Conference on Design, Construction and Operation of Nuclear Power Plants, Portland, Oregon, August 1984.

(5) L. Neymotin and P. Saha, "A Typical BWR/4 MSIV Closure ATWS Analysis Using RAMONA-3B with Space-Time Neutron Kinetics," Paper No. A3, proceedings of the International Nuclear Power Plant Thermal Hydraulics and Operations Topical Meeting, Taipei, Taiwan, October 22-24, 1984, ed. J. Chao and C. Chiu (ANS).

(6) B. Chexal, W. Layman and J. Healzer, "Reducing BWR Power by Water Level Control During an ATWS: A Quasi-Static Analysis," EPRI Report, NSAC-69, May 1984.

(7) C.E. Peterson, et al., "Reducing BWR Power by Water Level Control During an ATWS: A Transient Analysis," EPRI Report, NSAC-70, August 1984.

(8) B. Chexal and W. Layman, "Reducing BWR Power by Water Level Control," Paper No. A2, Proceedings of the International Nuclear Power Plant Thermal Hydraulics and Operations Topical Meeting, Taipei, Taiwan, October 22-24, 1984, ed. J. Chao and C. Chiu (ANS).

(9) Wayne C. Jouse, "Sequence Matrix for the Analysis of an ATWS in a BWR/4; Phenomena, System and Operation of Browns Ferry Nuclear Plant Unit 1," INEL Draft Report, May 1984.

(10) R.M. Harrington and S. A. Hodge, "ATWS at Browns Ferry Unit One - Accident Sequence Analysis," NUREG/CR-3470, July 1984.

(11) C.J. Hsu and D.J. Diamond, "The Effect of Downcomer Water Level and Vessel Pressure on Boiling Water Reactor Power During an ATWS," BNL Draft Report, November 1984.

(12) W. Wulff, et al., "A Description and Assessment of RAMONA-3B MOD.0 Cycle 4: A Computer Code with Three-Dimensional Neutron Kinetics for BWR System Transients," NUREG/CR-3664, BNL-NUREG-51746, January 1984.

(13) A. Ahlin, et al., "A Fuel Assembly Burnup Program," AE-RF-76-4158, June 1978.

(14) D.J. Diamond, Ed. "BNL-TWIGL, A Program for Calculating Rapid LWR Core Transient," BNL-NUREG-21925, Brookhaven National Laboratory, 1976.

(15) P.Saha, G.C. Slovik and L.Y. Neymotin, "RAMONA-3B Calculations for the Browns Ferry ATWS Study," BNL-NUREG Report to be published.

(16) S. Borresen, "A Simplified Coarse-Mesh Three-Dimensional Diffusion Scheme for Calculating the Gross Power Distribution in a Boiling Water Reactor," Nuclear Science and Engineering 44(1971) 37-43.

(17) T. G. Theofanous, "Modeling of Basic Condensation Processes," presented at the WRSR Workshop on Condensation, Silver Spring, Maryland, May 24-25, 1979.

(18) J.H. Linehan, "Interaction of Two Dimensional, Stratified, Turbulent Air-Water and Steam-Water Flows," ANL-7444, May 1968.

(19) H.R. Connell, et al., "User's Manual for RAMONA-3B: A Computer Code with Three-Dimensional Neutron Kinetics for BWR System Transients", BNL Draft Report, February 1984.

NOMENCLATURE

a,b,c	coefficients used in rod controlled void feedback
a',b',c'	coefficients used in rod uncontrolled void feedback
c_i	delayed neutron precursor concentration, m^{-3}
D	diffusion coefficient, m
E	exposure
F	control fraction
f	friction factor
G_m	mixture mass flux, kg/m^2s
g	acceleration due to gravity, m/s^2
j	volumetric flux density, m/s
p	pressure (Pa)
P	$\delta\Sigma/\delta T_m$
g'_v	linear wall heating rate, W/m
q'''	gamma heating rate, W/m^3
R	$\delta\Sigma/\delta\sqrt{T_F}$
S	slip ratio
St	Stanton number
T_F	fuel temperature

T_m	moderator temperature
u	specific internal energy, J/kg
V	void history
v	velocity
v_o	bubble rise velocity, m/s

Greek

α	void fraction
β	total delayed neutron fraction
Γ_v	evaporation rate, $kg/m^3 s$
λ	decay constant for delayed neutrons, s^{-1}
Σ	macroscopic neutron cross section, m^{-1}
ϕ	neutron flux, $m^{-2}\ s^{-1}$
ϕ_m^2	two phase mixture friction multiplier
ρ	density, kg/m^3
ν	mean number of neutrons in fast or thermal group

Subscripts

1	*fast-group neutrons*
2	thermal-group neutrons
a	absorption
f	*fission*
g	vapor (saturated)
i	index for delayed precursor
ℓ	liquid
m	mixture

Abbreviations

HPCI	High Pressure Coolant Injection
MSIV	Main Steamline Isolation Valve
PSP	Pressure Suppression Pool
RCIC	Reactor Core Isolation Cooling
SRV	Safety Relief Valve
TAF	Top of Active Fuel
TVA	Tennessee Valley Authority

APPENDIX

Neutron kinetics and thermal hydraulics are the two major parts of the RAMONA-3B code. Heat generation and conduction in the fuel rod link them together. Figure 14 shows the coupling and interaction among these parts as employed in RAMCNA-3B.

Neutron Kinetics

The neutron kinetics model of RAMONA-3B starts from the following two-group, three-dimensional, time-dependent diffusion equations:

Fast Neutrons:

$$\frac{1}{v_2}\frac{\partial \phi_1}{\partial t} = \nabla \cdot D_1 \nabla \phi_1 - \Sigma_{21}\phi_1 - \Sigma_{a1}\phi_1 + (1-\beta)[\nu_1\Sigma_{f1}\phi_1 + \nu_2\Sigma_{f2}\phi_2] + \sum_{i=1}^{I} \lambda_i c_i \qquad \text{(A-1)}$$

Thermal Neutrons:

$$\frac{1}{v_2}\frac{\partial \phi_2}{\partial t} = \nabla \cdot D_2 \nabla \phi_2 + \Sigma_{21}\phi_1 - \Sigma_{a2}\phi_2 \qquad \text{(A-2)}$$

Delayed Precursors:

$$\frac{\partial c_i}{\partial t} = \beta_i[\nu_1\Sigma_{f1}\phi_1 + \nu_2\Sigma_{f2}\phi_2] - \lambda_i c_i \qquad \text{(A-3)}$$

where i = 1 to I (I < 6).

However, in RAMONA-3B, it is assumed that the thermal neutron leakage term, i.e., $\nabla \cdot D_2\nabla\phi_2$, can be either neglected or assumed to be constant. Thus, RAMONA-3B uses the well-known 1-1/2 group, coarse mesh diffusion model (16). The boundary conditions at the core periphery are specified with parameters related to the extrapolation length for the fast flux and the albedo for the thermal flux.

The three-dimensional power generation is the sum of prompt and delayed energy deposition rates.The prompt component is proportional to the instantaneous fission rate, whereas the delayed energy deposition rate is calculated from the 1979 ANS Standard 5.1 for decay heat. The cross section dependence on fuel and moderator temperatures, void fraction, boron concentration and control rod positions is taken into account in the neutron kinetics calculation.

Heat Conduction in Fuel Rod

Thermal energy storage and heat conduction in the fuel elements (pellet, gas gap and cladding) are computed using the following discrete-parameter model:

$$\rho c \frac{\partial T}{\partial t} = \nabla \cdot k\nabla T + q''' \qquad \text{(A-4)}$$

No axial conduction is allowed; heat capacities (ρc) in the pellet and cladding, along with the thermal conductivity in the cladding, are assumed to be constants. The gas gap conductance is a function of pellet temperature.

Thermal Hydraulics

The reactor vessel thermal-hydraulics model of RAMONA-3B starts from the following one-dimensional, four-equation model:

Vapor Mass:

$$\frac{\partial}{\partial t}(\alpha\rho_g) + \nabla \cdot (j_g\rho_g) = \Gamma_v \qquad \text{(A-5)}$$

Mixture Mass or Volumetric Flux:

$$\nabla \cdot j_m = \frac{\rho_\ell - \rho_g}{\rho_\ell\rho_g}\Gamma_v - \left[\frac{\alpha}{\rho_g}\frac{D_g\rho_g}{Dt} + \frac{(1-\alpha)}{\rho_\ell}\frac{D_\ell\rho_\ell}{Dt}\right] \qquad \text{(A-6)}$$

Mixture Momentum

$$\frac{\partial G_m}{\partial t} + \frac{\partial}{\partial Z}\left[\alpha\rho_g v_g^2 + (1-\varepsilon)\rho_\ell v_\ell^2\right] = - \frac{\partial p}{\partial Z} - g\rho_m - f_\ell \phi_m^2 \frac{G_m|G_m|}{2\rho_\ell D_h} \quad \text{(A-7)}$$

Mixture Energy:

$$\frac{\partial}{\partial t}\left[\alpha\rho_g u_g + (1-\alpha)\rho_\ell u_\ell\right] + \frac{\partial}{\partial Z}\left[\alpha\rho_g v_g h_g + (1-\alpha)\rho_\ell v_\ell h_\ell\right] \frac{q'_w}{A} + q'''(1-\alpha) \quad \text{(A-8)}$$

Two further simplifications are made before the above set of equations is solved in RAMONA-3B. First, the mass and energy equations for the entire reactor vessel are combined (along with equations of state) to yield an equation for the average vessel pressure. Second, the momentum equations are integrated through each of the parallel channels in the core to obtain a number of closed-contour integral momentum equations. These equations along with the volumetric flux equations, i.e., Equation (A-6), are solved first to calculate the flow field in the entire vessel. The vapor mass and mixture energy equations, i.e., Equations (A-5) and (A-8), are then solved to calculate the void fractions and liquid temperatures in the vessel. These simplifications reduce the computation burden of RAMONA-3B without significant loss in accuracy.

The code uses a slip model of the form:

$$v_g = S\, v_\ell + v_o \quad \text{(A-9)}$$

to calculate the relative velocity between the vapor and liquid phases. Non-equilibrium vapor generation and condensation are accounted for through appropriate correlations. However, the vapor phase is assumed to be at saturation, while the liquid phase can be either subcooled, saturated or superheated. Appropriate correlations are also used for wall friction, form losses and wall heat transfer, including the post-CHF regime. The recently developed and implemented additional condenstion model is designed to predict the condensation rate when the subcooled water (either feedwater or ECCS water), injected through the feedwater sparger, enters the steam environment in the upper part of the downcomer region of a BWR/4 type reactor. The injected water enters the downcomer in the form of horizontal jets produced by the feedwater sparger nozzles, and then mixes with the saturated water exiting from the steam separators. The mixed water flows downward along the standpipes and along the upper plenum and core shroud in the form of a film. The condensation rate is calculated both on the liquid jets and on the liquid film.

The condenstion heat transfer, on a single subcooled liquid jet of diameter D, can be calculated using the correlation for the Stanton number following (17):

$$St_j = 0.02\ (L/D)^{-0.5}. \quad \text{(A-10)}$$

The second part of the present model accounts for condensation on the downflowing mixture composed of the original jet water, the newly formed condensate carried by the jets, and the saturated liquid exiting from the steam separators. The film velocity is assumed to be equal to the free-fall velocity, and the average film thickness is calculated through the flow rate and film velocity. A constant value of 0.0073 is used for the Stanton number following (18) for the condensation on the liquid films.

The code also uses a boron transport equation. However, boron is assumed to move with the liquid velocity, and no boron stratification in the lower plenum is allowed at this time.

The code employs models for typical BWR components, namely, jet pump, recirculation pump, steam separator and steam line with all necessary valves. However, all recirculation loops and steam lines are lumped together to one recirculation loop and one steam line, respectively. The code also tracks the two-phase mixture and collapsed water levels in the reactor vessel downcomer. The latter is used to activate some of the control and safety systems. For the steam line, it uses the mass and momentum equations with the assumption of an adiabatic process. Note that the steam line pressure is a function of both time and space. Therefore, the acoustic effects in the steam line due to valve closure and/or opening are taken into account.

Solution Method

In RAMONA-3B, all partial differential equations are first transformed into ordinary differential equations. The initial or steady-state conditions are then obtained by setting the time derivatives to zero, and iterating to calculate the eigenvalues of the system of equations. For the transient calculation, different methods are used for the different parts of the code. Specifically, the Gauss-Seidel iteration is used to integrate the fast neutron equations, explicit integration for delayed neutron equations, an iterative predictor-corrector method for heat conduction, the explicit first-order Euler method for vessel thermal hydraulics, and finally, the fourth-order Runge-Kutta-Simpson method for the steam line dynamics. The neutron kinetics and fuel heat conduction equations are integrated with a master time step, whereas the thermal-hydraulic equations use a substep. There are several time step controls to assure stability and accuracy of the calculation. The details of the RAMONA-3B code can be found in References (12 and 19).

TABLE 1. STEADY-STATE NOMINAL OPERATING CONDITIONS

Thermal Power, MWt	3198
Pressure, Pa	6.92×10^6
Mass Flow Rate of Coolant at:	
Core Entrance, kg/sec	12870
Steam Line/Feedwater, kg/sec	1592
Feedwater Temperature, °C	191.2
Core Inlet Subcooling, °C	11.5
Core Bypass Flow/Total Core Inlet Flow, %	10.6
Recirculation Drive Flow, kg/sec	4304

TABLE 2. SEQUENCE OF EVENTS

EVENT	(sec)
MSIV closure starts	0.0
S/RVs start to open	2.54
Recirculation pumps trip	3.7
MSIVs are completely closed	5.0
Maximum core averaged fuel temperature is reached (773°C)	4.5
Maximum system pressure (8.72 MPa) is reached	8.5
HPCI and RCIC injection activated	20.2
Operator assumes control	150.0
a) Water level dropped and maintained at TAF	
b) Reactor pressure vessel is depressurized according to PSP heat capacity temperature limit curve	
c) HPCI suction switched to PSP	538.0

TABLE 3. SAFETY AND RELIEF VALVES SET POINTS

Bank #	1 (4 Relief)	2 (4 Relief)	3 (3 Relief)	4 (2 Safety)
High Pressure (opening), 10^5Pa	77.22	77.91	78.60	87.22
Delay Time (opening), sec	0.0	0.0	0.0	0.0
Low Pressure (closing), 10^5Pa	73.77	74.46	75.15	83.77
Delay Time (closing), sec	0.0	0.0	0.0	0.0
Total Rated Flow (kg/sec)	108.64	108.64	81.48	54.32

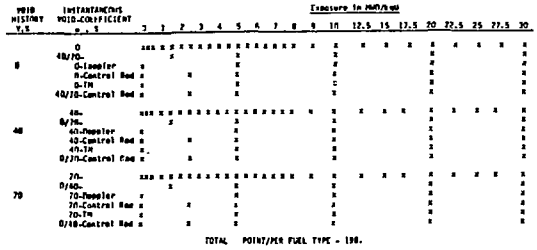

FIGURE 1. TVA - BROWNS FERRY 3 CYCLE 5 CASMO STATE POINTS FOR EACH FUEL TYPE

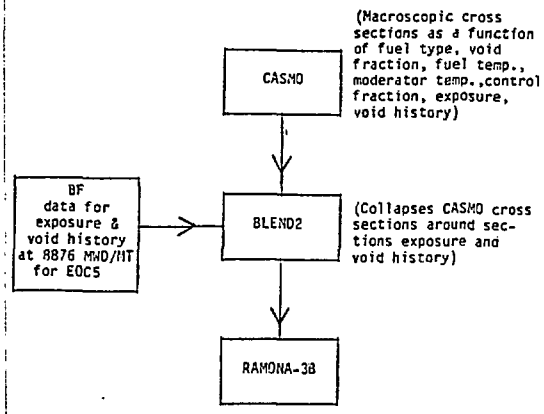

FIGURE 2. GENERATION OF BROWNS FERRY (BF) EOC-5 CROSS SECTIONS

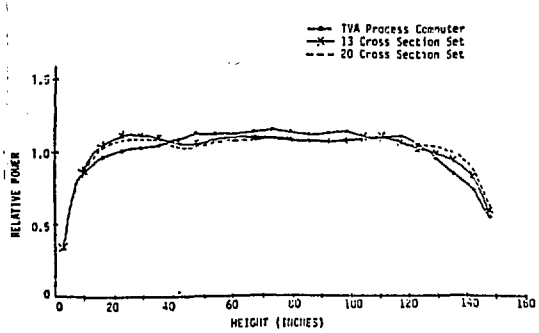

FIGURE 3. STEADY STATE PREDICTIONS WITH TWO DIFFERENT CROSS SECTION SETS

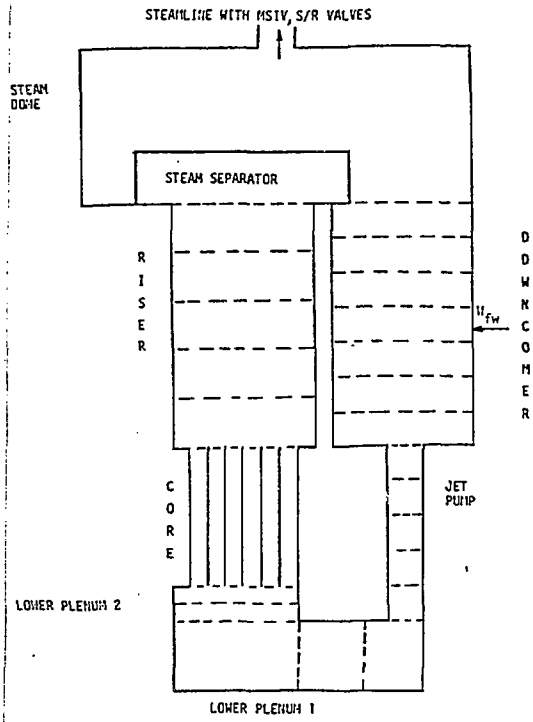

FIGURE 4. RAMONA-3B REPRESENTATION OF A BOILING WATER REACTOR VESSEL

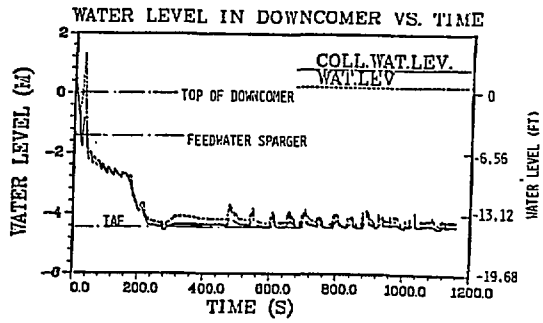

FIGURE 5. WATER LEVEL IN DOWNCOMER VS TIME

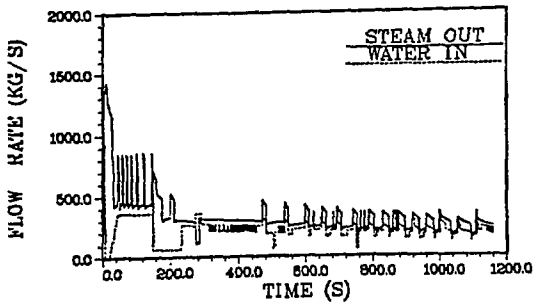

FIGURE 6. SRV AND FEEDWATER SPARGER FLOW RATE VS TIME

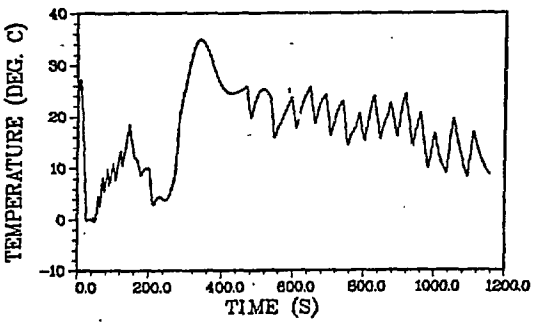

FIGURE 7. CORE INLET SUBCOOLING VS TIME

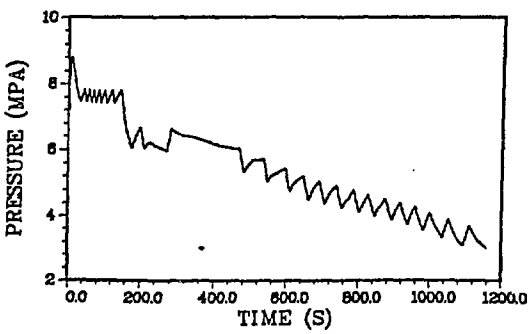

FIGURE 8. STEAM DOME PRESSURE VS TIME

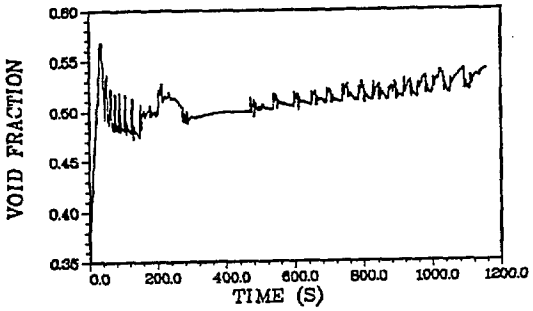

FIGURE 9. CORE AVERAGE VOID FRACTION VS TIME

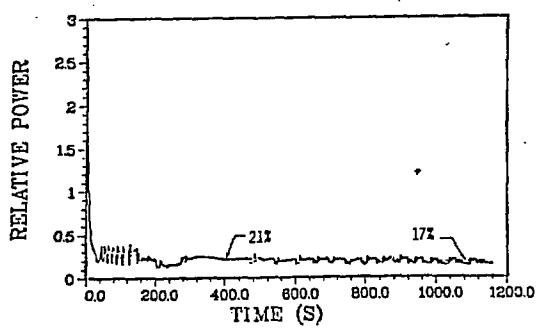

FIGURE 10. TOTAL REACTOR POWER VS TIME

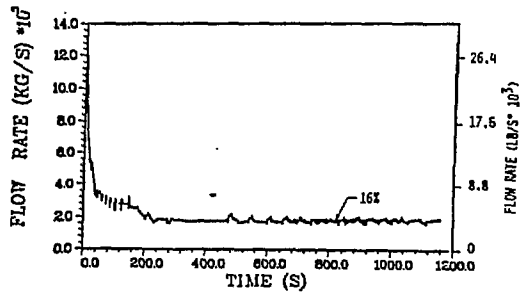

FIGURE 11. TOTAL CORE INLET FLOW RATE VS TIME

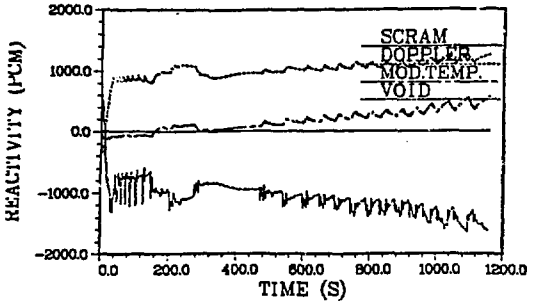

FIGURE 12. MAJOR CORE REACTIVITY COMPONENTS VS TIME

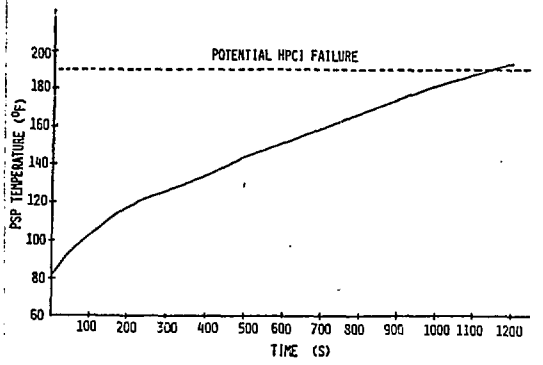

FIGURE 13. PRESSURE SUPPRESSION POOL BULK TEMPERATURE VS TIME

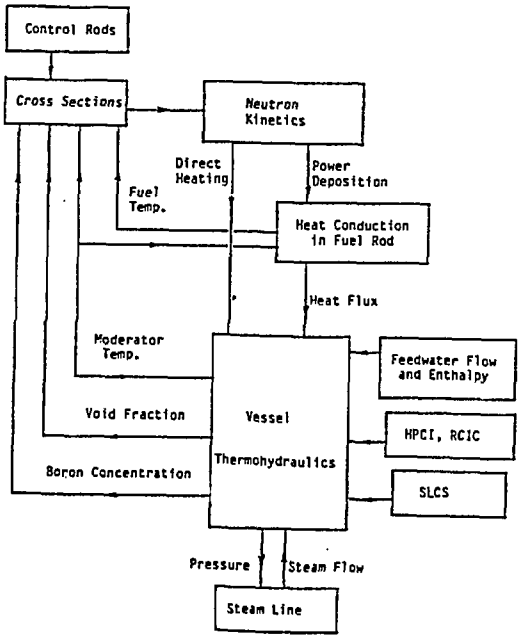

FIGURE 14. SIMPLIFIED FLOWCHART OF RAMONA-3B CALCULATIONAL LOGIC

DISCLAIMER